

# Ring-Pattern Dynamics in Smectic-C\* and Smectic-C<sub>A</sub>\* Freely Suspended Liquid Crystal Films

D. R. Link, L. Radzihovsky, G. Natale, J. E. MacLennan, and N. A. Clark  
*Condensed Matter Laboratory, Department of Physics, University of Colorado, Boulder, CO 80309 USA*

M. Walsh, S. S. Keast, and M. E. Neubert  
*Liquid Crystal Institute, Kent State University, Kent, OH 44242 USA*  
 (July 14, 2018)

Ring patterns of concentric  $2\pi$ -solitons in molecular orientation, form in freely suspended chiral smectic-C films in response to an in-plane rotating electric field. We present measurements of the zero-field relaxation of ring patterns and of the driven dynamics of ring formation under conditions of synchronous winding, and a simple model which enables their quantitative description in low polarization DOBAMBC. In smectic C<sub>A</sub>\* TFMHPOBC we observe an odd-even layer number effect, with odd number layer films exhibiting order of magnitude *slower* relaxation rates than even layer films. We show that this rate difference is due to much larger spontaneous polarization in odd number layer films.

Smectic liquid crystal phases are one-dimensional (1d) crystals consisting of a periodic stack of two-dimensional (2d) liquid layers. This rigidity allows them to be drawn into stable freely suspended films, integer numbers of smectic layers thick. In tilted smectic phases, the rod-shaped molecules, their long axes on average pointing along  $\mathbf{n}$ , strongly prefer to make an angle  $\theta_0$  with the layer normal  $\mathbf{z}$ , but have no energetic preference for the global azimuthal orientation of  $\mathbf{n}$  about  $\mathbf{z}$ . Consequently in these tilted phases, this azimuthal low energy degree of freedom can be described by a 2d unit director field,  $\mathbf{c}(x, y)$ , well correlated between layers and pointing along the projection of  $\mathbf{n}$  onto the smectic layer, as shown in Fig. 1.

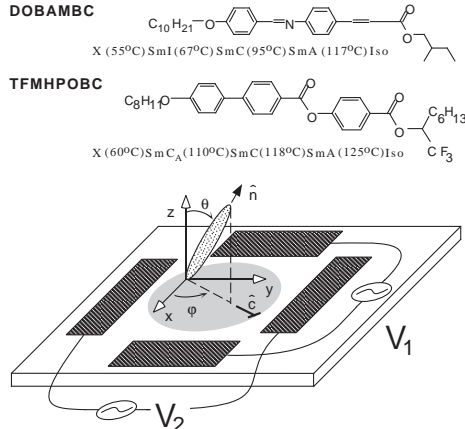


FIG. 1. Chemical structures and phase diagrams for DOBAMBC and TFMHPOBC, and geometry for molecules in a tilted smectic phase. The projection of the director  $\mathbf{n}$  onto the  $x-y$  plane defines the  $\mathbf{c}$ -director ( $\dashv$ ). Freely suspended smectic liquid crystal films are drawn over a hole in a glass coverslip. An in-plane rotating electric field is applied to the films by applying out-of-phase sinusoidal voltages,  $V_1$  and  $V_2$ , to electrodes placed around the hole as shown. The  $\mathbf{c}$ -director is visualized with depolarized reflected light microscopy.

In chiral smectics, symmetry demands an in-plane polarization  $\mathbf{P}(x, y)$  to be present, either along (longitudinal) or perpendicular (transverse) to  $\mathbf{c}(x, y)$ , depending on the details of the tilted smectic phase and the number of smectic layers in the film [1–3]. Consequent coupling of the director  $\mathbf{c}(x, y)$  to an in-plane applied electric field has enabled several key optical experiments on freely suspended films ranging from light scattering [4] and microscopy [5] to the determination of ground state structure of novel liquid crystal phases [3].

In these experiments, in order to prevent flow instabilities, the direction of the in-plane aligning electric field must be reversed at a frequency of 0.1 to 10 Hz. This process, still not well understood, typically leads to the formation of beautiful concentric ring patterns consisting of  $2\pi$ -walls in  $\mathbf{c}(x, y)$ , which can be imaged via Depolarized Reflected Light Microscopy (DRLM). A particular dark or light region of a DRLM image has a  $\mathbf{c}$ -director  $\mathbf{c}(x, y) = [\cos(\varphi(r)), \sin(\varphi(r))]$  of constant azimuthal orientation  $\varphi$ . Thus, with  $\varphi(r)$  pinned at the outer radius of the film and monotonically increasing toward the center of the film, rings appear. These distinctive ring patterns in  $\mathbf{c}$  were first studied quantitatively by Cladis et al. [6], who generated them mechanically by rotating a needle inserted into the center of a smectic-C (SmC) film. Later it was reported that ring patterns could be produced in ferroelectric films by applying a *rotating* (rather than bipolar) in-plane electric field  $\mathbf{E}(t)$  [7], with the first systematic experimental study mapping out the ring-pattern formation phase diagram given in Ref. [8]. Despite significant experimental attention there has only been *qualitative* theoretical understanding of ring-pattern formation and relaxation dynamics. Here we present a simple model, which enables quantitative understanding of E-field wound ring-pattern dynamics and subsequent

zero field ring unwinding relaxation. We find excellent agreement with our experiments on the low polarization ( $P \sim 3 \text{ nC/cm}^2$ ) SmC\* DOBAMBC [9]. However, our experiments on smectic-C<sub>A</sub>\* TFMHPOBC [10] reveal a novel odd-even smectic layer effect, with order of magnitude slower relaxation times in the high polarization odd layer number films and large ring distortion, driven by bend/splay elastic anisotropy ( $P \sim 75/N \text{ nC/cm}^2$ , where  $N$  is an odd number of smectic layers). These latter observations lie beyond our model and their quantitative description most certainly requires understanding of screening-ion dynamics.

The free energy density of the 2d nematic orientation field  $\mathbf{c}(x, y)$  of a freely suspended film in an applied field is given by

$$f(x, y) = \frac{K_S}{2}(\nabla \cdot \mathbf{c})^2 + \frac{K_B}{2}(\hat{\mathbf{z}} \cdot \nabla \times \mathbf{c})^2 - \mathbf{E} \cdot \mathbf{P} \quad (1)$$

where the first two terms are the energies of splay and bend of  $\mathbf{c}$  with 2d elastic constants  $K_S$  and  $K_B$ , respectively, originating from the 3d Frank free energy for  $\mathbf{n}$ . The last term is the electric field director aligning energy, acting through the polarization field density  $\mathbf{P}$ , which we take to be rigidly locked to the  $\mathbf{c}$  director, and for purposes of this development, orthogonal to  $\mathbf{c}$ .

Assuming simple relaxational dynamics for  $\mathbf{c}$ , with a viscous damping coefficient  $\gamma$ , and taking  $K_S \approx K_B \equiv K$  (but see below), we obtain an equation of motion for  $\varphi(x, y, t)$ ,

$$\gamma \frac{\partial \varphi}{\partial t} = K \nabla^2 \varphi - PE \sin(\varphi - \omega_e t). \quad (2)$$

In above, we have taken  $|\mathbf{P}| \equiv P$  and  $|\mathbf{E}| \equiv E$  to be constants and the electric field rotating at frequency  $\omega_e$  in the  $x$ - $y$  plane. Eq. 2 quite clearly ignores the dipolar interaction and the rich 2d liquid hydrodynamics coupled to the  $\mathbf{c}$  director, which can in principle become important under conditions of strong drive. Despite these shortcomings, as we will show below, most of our experimental data on ring patterns dynamics in the low  $P$  liquid crystals is *quantitatively* described by this model. Its extension to treat observations in high polarization materials will be a subject of a future publication [11].

A detailed analysis of Eq. 2 predicts a ring formation phase diagram in the applied  $E$ -field strength and winding frequency  $\omega_e$  space, which is consistent with our experimental observations. The dynamics is simplest in the regime of large  $E \gg E_c \equiv U_s/P$  and small  $\omega_e \ll \omega_c \equiv PE/\gamma$ , in which the areal  $\mathbf{c}$ -director field alignment torque  $PE$  is much larger than *both* the pinning energy (torque)  $U_s$  of  $\mathbf{c}$  at the outer boundary (radius  $R$ ) of the film, and the frictional torque  $\gamma\omega_e$ . In this regime the director field  $\mathbf{c}$  is *uniform*, synchronously following (at frequency  $\omega = \omega_e$ ) the rotating field  $\mathbf{E}$ , with a constant phase lag  $\delta = \sin^{-1}(\omega_e/\omega_c)$ , set by the balance

between the  $E$ -field alignment and frictional torques. Clearly, for  $\omega_e > \omega_c$  this synchronous metastable solution, corresponding to the areal alignment of  $\mathbf{P}$  along  $\mathbf{E}$  is unstable to a uniform asynchronous dynamical regime, in which the director  $\mathbf{c}$  uniformly winds at a rate  $\omega$  smaller than  $\omega_e$  of the rotating  $E$ -field. Away from the actual transition into this asynchronous regime, the dynamics can be explicitly worked out perturbatively in  $\omega_c/\omega_e$  and we find that in addition to fast oscillatory dynamics at harmonics of the “washboard” frequency  $\omega_e$ , the spatially uniform phase  $\varphi(t)$  advances *linearly* in time, on average, with frequency  $\omega = \frac{1}{2}\omega_e(\omega_c/\omega_e)^2 \ll \omega_e$ , which, interestingly, *decreases* with  $\omega_e$ . Obviously, no rings are produced in these two high  $E$ -field regimes.

Ring winding regimes lie in the range of low applied  $E$  fields, such that the pinning at the outer boundary (at  $R$ ) is stronger than the areal alignment torque  $PE$ . To analyze the synchronous,  $\omega_e < \omega_c$ , ring winding dynamics, we take  $\varphi(\mathbf{r}, t) \equiv \tilde{\varphi}(\mathbf{r}, t) + \omega_e t$ , and look for azimuthally symmetric traveling solution for  $\tilde{\varphi}(\mathbf{r}, t) \equiv \vartheta(r - vt)$ , which satisfies

$$\xi^2 \ddot{\vartheta} + \frac{v}{\omega_c} \dot{\vartheta} = \sin \vartheta + \frac{\omega_e}{\omega_c}, \quad (3)$$

where “dot” indicates differentiation with respect to the argument  $r - vt$ ,  $\xi \equiv \sqrt{K/PE}$ , and we have, for now, neglected the term  $\xi^2 \dot{\vartheta}/r$  that is subdominant for large rings. The boundary condition  $\varphi(R, t) = \varphi_0$  translates into  $\vartheta = \varphi_0 - \omega_e t$  and feeds in  $2\pi$ -solitons (winds rings) at a rate  $\omega_e$  from the outer boundary  $r = R$  of the film (see Fig. 2(a)).

Rings are traveling soliton solutions to the above equation, which can be found by noting the isomorphism of the Eq. 3 with the Newtonian dynamics of a particle of mass  $\xi^2$ , friction coefficient  $v/\omega_c$  moving down a (unit strength) sinusoidal potential under an external force  $\omega_e/\omega_c$ . First we note that, without winding, a radial profile of an isolated ( $\omega_e = 0$ ) ring of radius  $r_0$  can be determined in closed form and is given by a well-known soliton solution  $\vartheta(r) = 4 \arctan [e^{(r-r_0)/\xi}]$ . It corresponds to the motion of a fictitious particle between two maxima (at 0 and  $2\pi$ ) of the potential  $V(\vartheta) = 1 - \cos \vartheta$  *without* external force and therefore a vanishing friction coefficient. Consequently, without winding, an isolated ring is stationary,  $v = 0$ . This stationary  $\omega_e = 0$  solution can be easily extended to a concentric periodic array of rings  $d$  apart, by choosing the “total energy”  $E$  and therefore the initial “kinetic energy”,  $\xi^2(\dot{\vartheta})^2/2$ , such that the effective particle can travel between maximas in “time”  $d$ . Although the solution can be expressed in terms of special functions, the only features of it that are important to us is its sigmoidal shape, the ring’s radial width  $\xi$  and  $\dot{\vartheta}|_{2\pi n} \approx 2\pi/d$ .

For a finite synchronous winding rate,  $\omega_e \neq 0$ , the fictitious particle is under an external constant force  $\omega_e/\omega_c$ , leading to a tilted periodic potential. The mapping of the

ring winding problem onto particle dynamics makes it immediately clear that in this case, a solution of a *periodic* array of self-similar concentric rings is only possible if the fictitious particle moves in the presence of a *unique* value of the frictional coefficient  $v/\omega_c$ . This value is determined by the condition that the “energy”  $2\pi\omega_e/\omega_c$ , gained by the particle from descending to a next local potential maximum is precisely the energy  $v/\omega_c \int_{\vartheta_0}^{\vartheta_0+2\pi} d\vartheta \dot{\vartheta}$  dissipated due to “friction”. This condition predicts that, even in the absence of tension, rings wound at rate  $\omega_e$  *must* move toward the center with velocity  $v \approx (\pi/4)\omega_e\xi$ , a result that can also be clearly seen from noting that the  $2\pi$ -soliton shifts by its width  $\xi$  at frequency  $\omega_e$ , the rate of rotation of the **c**-director (see Fig. 2(a)).

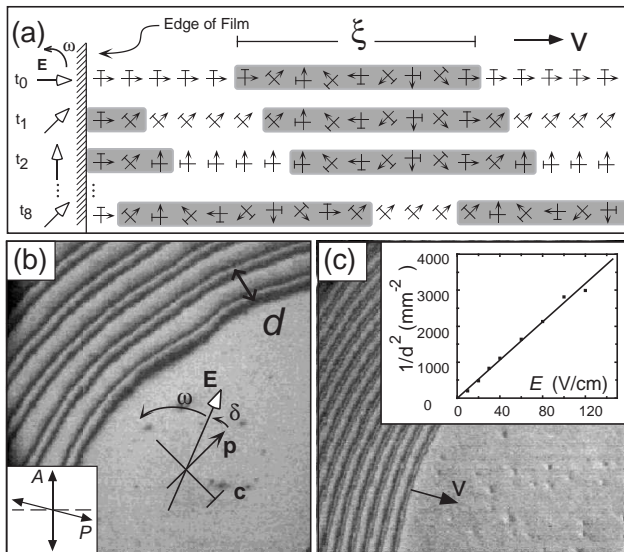


FIG. 2. Synchronous-winding ring patterns. (a) At the edge of the film, boundary conditions prevent **c** from rotating with the field resulting in the generation of a new  $2\pi$ -soliton ring with every revolution of the field. A one dimensional  $2\pi$ -wall (shaded region) in a rotating electric field **E** moves with a constant velocity proportional to its width and rotation frequency of the field. (b) Photomicrograph of the development of a ring pattern ( $E = 30$  V/cm). The separation between rings  $d$  is independent of the frequency of rotation  $\omega$  in the accessible frequency range (0.1 to 10 Hz). In (c)  $E$  is increased by a factor of four ( $E = 120$  V/cm) reducing  $d$  by a factor of two. The inset in (c) shows the expected linear dependence of  $1/d^2$  as a function of field strength.

In the time  $\tau_e = 2\pi/\omega_e$  that it takes a new soliton ring to be created at the outer film edge  $R$ , rings created before it, move toward the center of the film a distance  $d = v\tau_e = (\pi^2/2)\xi$ , predicting a steady state pattern of evenly spaced (by  $d$ ), moving, concentric rings, as illustrated in Fig. 2(b, c). As shown in the inset of Fig. 2(c), our experiments indeed find  $d^2 \propto 1/E$  in agreement with the above theoretical prediction for  $d$  and  $\xi$ . We also, however, find that rings spacing increases toward the center of the film, inconsistent with the above  $r$ -independent

prediction for  $d$ . It is easy to show that this deviation is due to the increased importance (at small  $r$ ) of the ring line tension, contained in the  $\xi^2 \dot{\vartheta}/r$  term, neglected in the Eq. 3. Line tension contributes an additional  $E$ -independent velocity  $\delta v_\tau = dr/dt = -K/(\gamma r)$  that must be superimposed on the velocity due to the rotating field [5], and predicts a parabolic spacing of soliton rings in the central region.

Contrary to the observations of Dascalu et al. [12] experimentally we find both synchronous ( $\omega < \omega_c$ ) and asynchronous ( $\omega > \omega_c$ ) winding of ring patterns. However, in contrast to the well-defined soliton-like rings of width  $\xi$  wound in the synchronous,  $\omega_e < \omega_c$  regime discussed above, in the asynchronous,  $\omega_e > \omega_c$  regime, the rings are not solitons and their width is roughly set by  $R/n(t)$ , decreasing as their number  $n(t)$  grows with frequency  $\omega = \frac{1}{2}\omega_e(\omega_c/\omega_e)^2$ . We have confirmed experimentally our prediction of the linear  $E$ -field dependence of the critical frequency  $\omega_c$ , separating these two ring winding regimes.

We now turn our attention to ring unwinding dynamics at  $E = 0$ . We find that, in contrast to previous claims in the literature [6] a general solution for the relaxation is given by

$$\varphi(r, t) = \sum_n A_n J_0\left(\frac{a_n r}{R}\right) e^{-t/\tau_n}, \quad (4)$$

where  $\tau_n = (\gamma/K)(R/a_n)^2$  is the time constant for  $n$ th mode,  $a_n$  are the zeros of the zeroth order Bessel function  $J_0(r)$ , and  $A_n$  are completely determined by the initial condition  $\varphi(r, 0)$ . Since higher order ( $n > 1$ ) terms relax with a larger time constant than lower order terms,  $\varphi(r, t)$  rapidly takes on the shape of the lowest  $n = 1$  term.

As a case study, we measured the relaxation of ring patterns in ferroelectric SmC\* DOBAMBC and antiferroelectric SmC<sub>A</sub>\* TFMHPOBC. Having determined  $A_n$ 's from the initial measured  $E = 0$   $\varphi(r, 0)$  director profile, the subsequent evolution of  $\varphi(r, t)$  is completely specified by Eq. 4. As we show in Fig. 3, our theoretical prediction for  $\varphi(r, t)$  is in excellent agreement with the experimentally determined evolution of the director profiles. These one parameter fits to experimental data allows us to quite accurately determine the important ratio  $\gamma/K$ . In a 5 layer film we find  $\gamma/K = 1.997 \times 10^5 \text{s/cm}^2$ , which, surprisingly, is an order of magnitude larger than the previously reported value of  $1.4 \times 10^4 \text{s/cm}^2$  [5], for reasons that are still unclear to us.

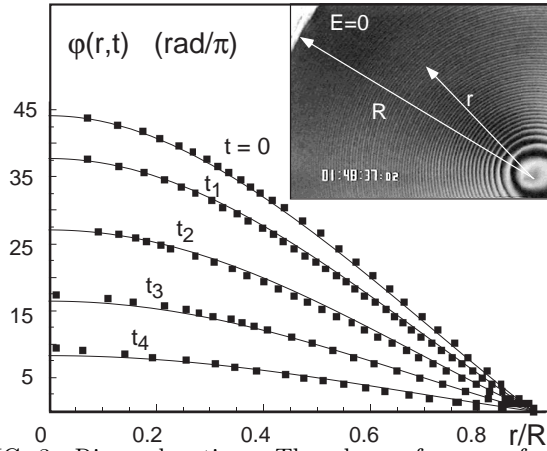


FIG. 3. Ring relaxation. The phase of  $\mathbf{c}$  as a function of  $r$  and  $t$  is shown (solid squares) for a five layer film of DOBAMBC during the relaxation process. The solid lines are fits to the first three terms of Eq. (4) using  $A_1 = 134.9$ ,  $A_2 = 0.29$ ,  $A_3 = 1.15$  and  $\gamma/K = 1.99 \times 10^5$  s/cm<sup>2</sup> at times  $t_1 = 41.8$ ,  $t_2 = 134.7$ ,  $t_3 = 275.1$  and  $t_4 = 467.4$  s. The inset is a typical video image of a film of radius  $R$  during relaxation.

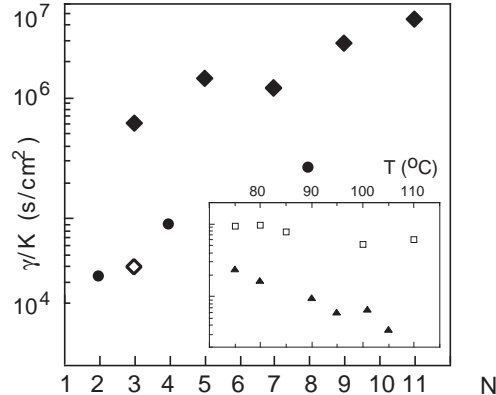


FIG. 4. Layer number dependence of  $\gamma/K$  in  $\text{SmC}_A^*$  TFMHPOBC. The effective ratio of  $\gamma/K$  for films of different number of layers shows a strong odd-even layer number dependence, with high polarization,  $N$ -odd films (solid diamonds) having a much larger ratio than the low polarization,  $N$ -even films (solid circles). The ratio in an  $N = 3$  film (open diamond) of nearly racemic  $\text{SmC}_A^*$  TFMHPOBC is similar to  $N$ -even films. The temperature dependence of  $\gamma/K$  is shown in the inset for three layer (open squares) and two layer (solid triangles) films.

Such quantitative measurements in  $\text{SmC}_A^*$  TFMHPOBC revealed an intriguing odd-even dependence of  $\gamma/K$  on layer number  $N$ . In these experiments the relaxation at the center of the pattern,  $\varphi(0, t)$  was recorded and fit to Eq. 4 and used to extract  $\gamma/K$ . The results shown in Fig. 4, reveal that  $N$ -odd films relax much more slowly than  $N$ -even films. The two main differences between  $N$ -odd and  $N$ -even films are that  $N$ -odd films have a large net transverse polarization, while  $N$ -even films have a significantly smaller net longitudinal polarization (in the tilt plane) [2]. To demonstrate that it is the difference in the magnitude of the polarization

between the odd and even layer films that is responsible for this novel effect, we measured the  $\gamma/K$  ratio via our ring relaxation technique in three-layer  $\text{SmC}_A^*$  films of almost-racemic TFMHPOBC (a small amount of chiral TFMHPOBC was added to racemic TFMHPOBC so that  $N$ -odd films would have a small net polarization). These low polarization odd-layer films display large  $\mathbf{c}$ -director fluctuations and ring pattern relaxation rates comparable to  $N = 2$  and  $N = 4$  films, and have an effective  $\gamma/K$  an order of magnitude lower than the enantiomerically pure material. This strong dependence on the magnitude of the spontaneous polarization indicates, that while Eq. 4 captures the essence of ring pattern relaxation, it is unable to account for the difference in the relaxation rates between small and large polarization materials. We note that the dynamics of low-polarization  $N$ -even films are described much better by Eq. 4 than those of high-polarization  $N$ -odd films. The temperature dependence of  $\gamma/K$ , however, is similar in both  $N$ -even and  $N$ -odd as is shown in the inset of Fig. 4.

This work by was supported by NSF grants DMR96-14061, DMR89-20147, DMR-9809555, DMR-9625111, NASA grant NAG3-1846, and DARPA contract MDA972-90C-0037. L.R. also acknowledges support by the A.P. Sloan and David and Lucile Packard Foundations.

- 
- [1] R. B. Meyer, L. Liebert, L. Strzelecki, and P. Keller, J. Phys. Lett. **36** L69 (1975).
  - [2] D. R. Link, J. E. Maclennan, N. A. Clark, Phys. Rev. Lett. **77**, 2237 (1996).
  - [3] D. R. Link, G. Natale, R. Shao, J. E. Maclennan, N. A. Clark, E. Körblova, and D. M. Walba, Science **278**, 1924 (1997);
  - [4] C. Y. Young, R. Pindak, N. A. Clark, and R. B. Meyer, Phys. Rev. Lett. **40**, 773 (1978).
  - [5] R. Pindak, C. Y. Young, R. B. Meyer, and N. A. Clark, Phys. Rev. Lett. **45**, 1193 (1980).
  - [6] P. E. Cladis, Y. Couder, and H. R. Brand, Phys. Rev. Lett. **55**, 2945 (1985).
  - [7] G. Hauck, and H. D. Koswig, Ferroelectrics **122** 253 (1991).
  - [8] G. Hauck, H. D. Koswig, and U. Labes, Liq. Cryst. **14** 991 (1993).
  - [9] D. S. Parmar and Ph. Martinot-Lagarde, Ann. Phys. **3**, 275 (1978).
  - [10] Y. Suzuki, T. Hagiwara, I. Kawamura, N. Okamura, T. Kitazume, M. Kakimoto, Y. Imai, Y. Ouchi, H. Takezoe, and A. Fukuda, Liq. Cryst. **6**, 167 (1989).
  - [11] D. R. Link and L. Radzihovsky, unpublished.
  - [12] C. Dascalu, G. Hauck, H. D. Koswig, and U. Labes, *16<sup>th</sup> International Liquid Crystal conference, Kent Ohio*, paper D4P.38 (1996).